MINERALOGIA POLONICA
Vol. 35, No 1, 2004
PL ISSN 0032-6267

Roman WŁODYKA[1], *Roman WRZALIK*[2]

APOPHYLLITE FROM THE MIĘDZYRZECZE SILL NEAR BIELSKO-BIAŁA, THE TYPE AREA OF THE TESCHENITE-PICRITE ASSOCIATION

A b s t r a c t . Fluorapophyllite crystals from complex veins crosscutting a small pectolite skarn body at the top of the Międzyrzecze sill were studied by means of chemical analysis, X-ray diffraction, thermal analysis and both infrared and Raman spectroscopy. The apophyllite from Międzyrzecze, lacking abnormal optical properties, is tetragonal with lattice parameters: a = 8.974(2) Å, c = 15.798(6) Å. DTA curves exhibit two endothermic peaks centred at about 330 and 430°C. The dehydration behaviour of apophyllite results from the development on the outer parts of grains of an amorphous layer. It forms a diffusion barrier that moderates H_2O migration and originates in the second endothermic peak. IR investigations showed a new stretching vibration ν(OH), not previously recognized in apophyllite. This new band at 3627 cm^{-1} can be attributed to ν(OH) of the hydroxyl group which substitutes for F^- in the apophyllite structure. Selective leaching of phlogopite probably released the elements necessary for apophyllite precipitation in open spaces of the fissures in the upper part of the picrite sill.

Key-words: fluorapophyllite, pectolite skarn, Międzyrzecze, the Polish Carpathians

INTRODUCTION

Apophyllite is a secondary mineral occurring in a variety of rock types affected by low-temperature water-rock interactions. There are two types of apophyllite occurrences: open-space filling and metasomatic. The first is closely associated with minerals such as calcite, quartz, prehnite, datolite, pectolite and both Ca- and Na-zeolites. Replacement of Ca-bearing minerals such as wollastonite, datolite and Ca-garnet by dissolution-reprecipitation processes (Borisenko 1982) gives rise to the second type. Apophyllite generally occurs as the last phase in most paragenetic sequences; typically, its temperature of crystallization ranges from 220 to120°C (Borisenko 1982) and possibly down to normal groundwater temperatures. The results obtained by Flaming et al. (1999) suggest that apophyllite can give geologically meaningful Rb-Sr and K-Ar ages for low-temperature hydrothermal events.

[1] University of Silesia, Faculty of Earth Sciences, ul. Będzińska 60, 41-200 Sosnowiec, Poland; e-mail: rwlodyka@wnoz.us.edu.pl

[2] University of Silesia, Faculty of Physics, ul. Uniwersytecka 4, 40-007 Katowice, Poland.

The chemical composition of apophyllite varies, especially with regard to the fluorine content. Dunn et al. (1978) redefined the apophyllite group as a solid-solution series between hydroxyapophyllite, $KCa_4Si_8O_{20}(OH,F) \cdot 8H_2O$ [where (OH)X>>F] and fluorapophyllite, $KCa_4Si_8O_{20}(F,OH) \cdot 8H_2O$ [where (OH)<<F]. The sodium analogue, $NaCa_4Si_8O_{20}F \cdot 8H_2O$, was described by Matsueda et al. (1981). A continuous pseudo solid solution series between the Na- and K-varieties of fluorapophyllite was recognized by Matsueda et al. (1981) and Miura et al. (1981). Substitution of K^+ (up to 25 %) by NH_4^+ occurs in ammonian apophyllites (Marriner et al. 1990).

The apophyllite structure was determined by Taylor and Náray-Szabo (1931). Subsequent refinements by Colville et al. (1971), Chao (1971) and Pechar (1987) confirmed the early results. The apophyllite is an unusual hydrous, sheet-structured mineral. It consists of infinite silicate $(Si_2O_5)^{2-}$ layers parallel to (001) that comprise 4- and 8-membered rings. These puckered silica sheets are linked together through Ca^{2+} and K^+ coronation of O atoms and hydrogen bondings (Ca, K and F/OH sheets). K^+ coordinates eight water O atoms and Ca coordinates four silica-layer O ions, two water O ions and F^-.

Potassium apophyllite is normally tetragonal (*P4/mnc*) and shows no deviations from that system in X-ray analysis though some apophyllite crystals show abnormal optical properties (e.g., Sahama 1965). Their internal, biaxial domains with orthorhombic, monoclinic or triclinic symmetry were probably produced by an order-disorder growth mechanism (Akizuki et al. 1985).

The aim of this work is to describe the discovery of apophyllite crystals in the Polish segment of the Outer Carpathians, a classic type-area of the teschenite-picrite association. The presence of apophyllite was also noted in a Moravian quarry near Žermanice Dam (Kudělásek et at. 1987), where datolite together with calcite and apophyllite form up to 10 cm thick veins in diabase.

APOPHYLLITE OCCURRENCES

At the top of the picrite sill in Międzyrzecze Górne near Bielsko-Biała, a pectolite skarn occurs (Phot. 1). It is composed of pectolite crystals with poikilitic inclusions of Ti-garnets, diopside, natrolite and analcime. That small, 12 m thick sill consists of a high amount of olivine (up to 30 vol. %), phlogopite (up to 35 vol. %) and diopside (up to 25 vol. %). The lenticular endoscarn, up to 2 m thick, 5 m wide and 12 m long, is characterized by numerous veins ranging in thickness from a few mm to 30 cm. The apophyllite crystals described here were collected in the central part of complex veins, in miarolitic cavities within massive calcite associated with datolite, pectolite and strontianite. The apophyllite crystallized, as the last phase, on datolite basal pinacoid faces (Włodyka et al. 1998). Thinner (< 5 mm) veins are filled with apophyllite, calcite and rare analcime.

The apophyllite from the Międzyrzecze sill typically forms small, clear, colourless to turbid white crystals, up to 3 mm long, with three habit-modifying forms: {001}, {101} and {110} (Kostov 1975). Only two morphological modifications of apophyllite were

distinguished: bipyramidal and isometric. The bipyramidal type displays well-developed {101} bipyramides; {110} prisms are generally small. The {001} faces exhibit very rough and dull surfaces lacking any sign of growth steps (Phot. 2). The isometric apophyllite shows approximately equal development of all the forms mentioned.

The apophyllite from Międzyrzecze is optically uniaxial without any sign of the abnormal optical properties of biaxial fluorapophyllite (e.g., Akizuki et al. 1985; Sahama 1965). In vertical sections, at the right angle to the thin vein walls, bunches of dislocations with orientation perpendicular to apophyllite growth layers are seen in transmitting light (Phot. 3). The origin of this phenomenon is probably connected with the capture of solid or fluid inclusions by apophyllite crystals growing on uneven fissure surfaces.

METHODS

Chemical compositions for representative Międzyrzecze apophyllite crystals were determined using a Cameca SX-100 electron microprobe analyzer with a ZAF correction system (accelerating voltage 15 kV; sample current 15 nA). H_2O^+ was determined in a Penfield tube.

X-ray diffraction powder patterns were obtained using a Philips PW 3710 diffractometer with filtered CuK_α radiation (35 kV, 40 mA). Selected diffraction lines were measured with longer (10s) counting time and 0.01° steps to achieve high-precision estimates of the cell parameters. The experimental profiles were fitted with Pearson VII function using the ProFit program to obtain the position of the selected lines. For the calculation of lattice parameters and the indexing of peaks, the X´Pert Plus program was used.

Using a Derivatograf C (MOM Budapest), thermal analysis of the apophyllite was carried out on 500-mg, hand-ground samples, placed in five Pt discs in order to obtain quick removal of reaction gaseous products, at the following heating rates: 2.5, 5 and 10°C/min.

Mid- and far-infrared powder spectra were recorded with the 2 cm^{-1} spectral resolution (mean of 124 scans) on a FTS 6000 Bio-Rad spectrometer equipped with a nitrogen-cooled MCT detector. The Grams/386 computer program was used for curve fitting.

Raman spectra of apophyllite crystals were recorded using a Lab-Ram dispersive spectrometer and an OLYMPUS BX40 confocal microscope. Argon-ion laser light (514.5 nm) was used to excite the spectra. The power at the sample was less than 30 mW. The polarizer, half-wave plate and analyser were used to control incident and scattering polarization. In order to avoid undesirable Reyleigh lines, the scattered light was passed trough a holographic notch filter with a 100 cm^{-1} cut-off. The intensity was measured using a Peltie-cooled CCD detector (1048 × 256 pixels). The 520.5 cm^{-1} line of pure silica was used to calibrate the spectrometer.

For the Raman experiments, crystals of apophyllite showing perfect (001) cleavage and well-developed (110) faces were oriented as shown in Figure 1. The laboratory and

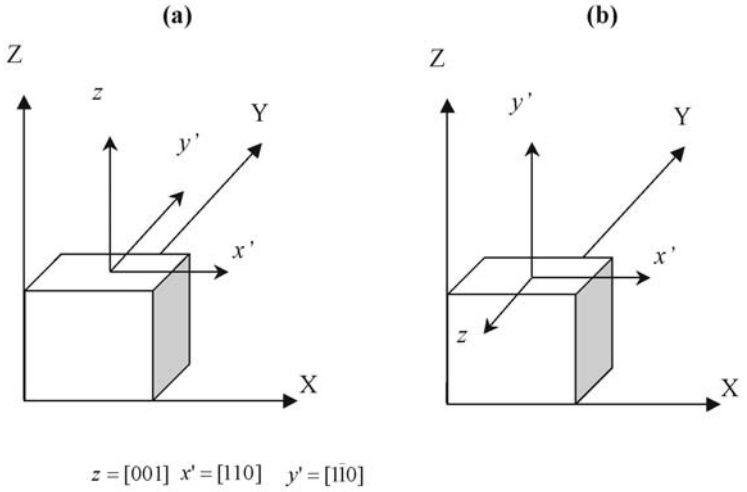

Fig. 1. Variations of cell dimensions with the fluorine content in fluorapophyllite.
X, Y, Z — laboratory frame, x′, y′, z — crystal directions

sample frames were as in the experiments of Adams et al. (1981). The incident light was propagated in the $\overline{Z}$ direction of the laboratory frame, whereas the scattered light was observed in the Z direction (0 degree scattering geometry). The polarization of the light beam is specified here by means of the Port's notation, e.g., $\overline{z}(\boldsymbol{y'y'})z$, where $\overline{z}$ is the direction of incident light; y' the direction of polarization of incident light; y' the direction of polarization of scattered light, and z the direction of scattered light. Micro-Raman measurements on apophyllite were performed in two geometries, i.e., with the Z laboratory axis parallel to the apophyllite c axis [$\overline{z}(\boldsymbol{y'y'})z$ and $\overline{z}(\boldsymbol{x'y'})z$ experiments] and parallel to the y axis [$\overline{\boldsymbol{y}}'(zz)\boldsymbol{y'}$ and $\overline{\boldsymbol{y}}'(\boldsymbol{x'z})\boldsymbol{y'}$ and experiments, see Fig. 1a, b].

RESULTS

In the classification of Dunn et al. (1978), the apophyllite from Międzyrzecze (Table 1) belongs to the class of fluorapophyllite [where (OH)<F)]; its chemical formula is $(K_{0.96}Na_{0.03})_{0.99}Ca_{3.96}(Si_{7.95}Al_{0.04}P_{0.03})_{8.02}O_{19.98}(F_{0.83}OH_{0.17})_{1.00} \cdot 8.02H_2O$. The substitutions of Al for Si and Na for K in the crystal structure are limited. Unlike the apophyllite described here, most optically anomalous apophyllites exhibit elevated contents of Al_2O_3, up to 5.8 wt.% (e.g., Belsare 1969; Borisenko 1982). Therefore, Al/Si ordering or O-H bond orientation on the growth surface may explain the abnormal optical features of apophyllite (Akizuki at al. 1985).

The Międzyrzecze apophyllite is tetragonal with the following lattice parameters: a = 8.974(2) (Å), c = 15.798(6) (Å) and V = 1272.190 (Å^3). X-ray data are listed in Table 2. There is a solid solution series between fluor- and hydroxyapophyllite (Dunn et al.

1978); the maximum fluorine content is about 3.2 wt.% (Borisenko 1982). Marriner et al. (1990) demonstrated linear relationships between *a* and *c* cell parameters and the fluorine content; both parameters decrease linearly with increasing replacement of $(OH)^-$ by F^-. The cell parameters of the Międzyrzecze apophyllite confirm these findings (Fig. 2). However, as seen in Figure 2, there are differences in the cell parameters

TABLE 1

Chemical composition (wt.%) and formulae of apophyllite from Międzyrzecze, based on 29 (O,OH,F)

SiO_2	Al_2O_3	CaO	Na_2O	K_2O	P_2O_5	F	H_2O	O for F	Total
52.34	0.21	24.34	0.10	4.95	0.21	1.72	16.00	0.72	99.25
Si	Al	Ca	Na	K	P	F	H		
7.949	0.038	3.961	0.029	0.958	0.027	0.826	16.211		

TABLE 2

X-ray powder data for apophyllite from Międzyrzecze

$2\Theta_{Cu}$	d[Å]	I/I_o [%]	hkl	$2\Theta_{Cu}$	d[Å]	I/I_o [%]	hkl
11.180	7.907	17	0 0 2	41.193	2.189	4	1 0 7
11.311	7.816	36	1 0 1	41.874	2.155	2	4 0 2
13.911	6.361	3	1 1 0	42.781	2.112	10	3 1 5
19.515	4.545	32	1 0 3	42.877	2.107	10	3 2 4
19.745	4.493	8	2 0 0	45.173	2.005	5	4 2 0
22.488	3.950	100	0 0 4	51.539	1.772	2	2 1 8
22.827	3.892	11	2 1 1	51.694	1.767	12	3 1 7
24.867	3.577	26	2 1 2	53.110	1.723	3	1 0 9
26.557	3.353	12	1 1 4	54.711	1.676	3	4 1 6
28.095	3.173	10	2 2 0	55.439	1.656	1	5 2 1
29.952	2.981	86	1 0 5	56.760	1.620	2	3 1 8
30.365	2.942	6	3 0 1	57.244	1.608	2	2 1 9
31.764	2.815	3	2 1 4	57.704	1.596	2	2 4 6
31.999	2.795	2	3 1 1	58.371	1.579	28	0 0 10
33.526	2.671	3	3 1 2	59.725	1.547	5	2 3 8
35.929	2.497	21	3 1 3	62.122	1.493	3	1 3 9
36.149	2.483	29	2 1 5	63.554	1.463	2	1 5 6
36.945	2.431	10	1 1 6	65.799	1.418	3	0 1 11
40.969	2.201	5	2 1 6	69.453	1.352	3	1 2 11

for hydroxyapophyllite presented by Marriner et al. (1990) and by Dunn et al. (1978). It is not clear why these differences are so great. The substitution of Na for K gives rise to a reduction of cell dimensions and also to a lowering of the symmetry from tetragonal to orthorhombic (Miura et al. 1981). Borisenko (1982) revealed a negative relationship between the H_2O^+ content and the K^+/V ratio associated with that substitution (V is the unit-cell volume).

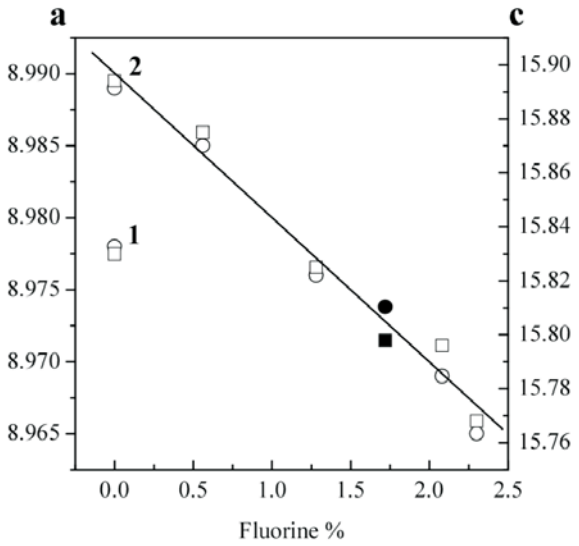

Fig. 2. Sample orientation and scattering configuration for Raman experiments.
Open circles — variation of the *a* parameter with fluorine content.
Open square — variation of the *c* parameter with fluorine content. Filled circle and square: fluorapophyllite from Międzyrzecze. Point 1 — data for hydroxyapophyllite (Dunn et al. 1978).
Point 2 — data for hydroxyapophyllite (Marriner et al. 1990)

Dehydration of apophyllite has been the subject of numerous studies. The majority of the apophyllite samples exhibit two distinct stages of weight loss (Fig. 4) corresponding to two endothermic peaks on the DTA curves (Fig. 3). In the literature, there are two models that describe this process. According to Marriner at al. (1990), the first stage of dehydration is connected with a loss of water molecules and results only in minor distortion of the apophyllite structure. The mineral breaks down into an amorphous material during the second stage. Ståhl et al. (1987) and Ståhl (1993) presented an alternative two-step reaction model. The first step leads to n (H_2O) = 7; after the expulsion of one water molecule from the $K^+(OH_2)_8$ polyhedron, the remaining water molecules assume a new crystallographic position preserving the tetragonal symmetry of apophyllite. Further water loss (the second step) results in the collapse of the Ca-K coordination and the formation of an amorphous material. In terms of this model, the second peak on the DTA curve can be explained as a kinetic, diffusion-controlled effect.

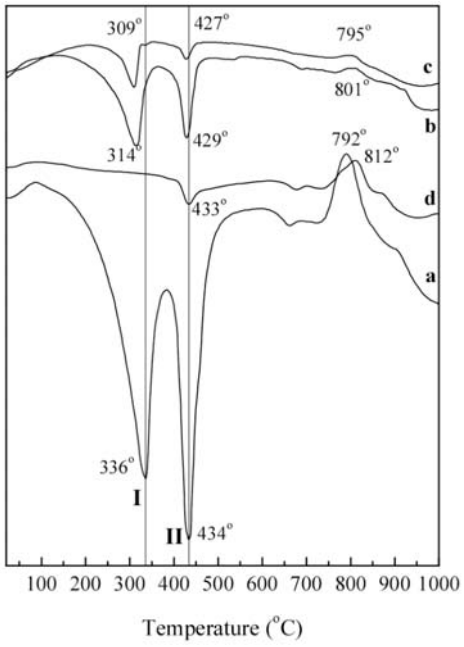

Fig. 3. Differential thermal curves of fluorapophyllite from Międzyrzecze obtained at the following heating rates in °C/min: a — 10, b — 5, c — 2.5 and d — 5.
The sample used for run *d* was previously isothermally heated at 280°C for 27 hours

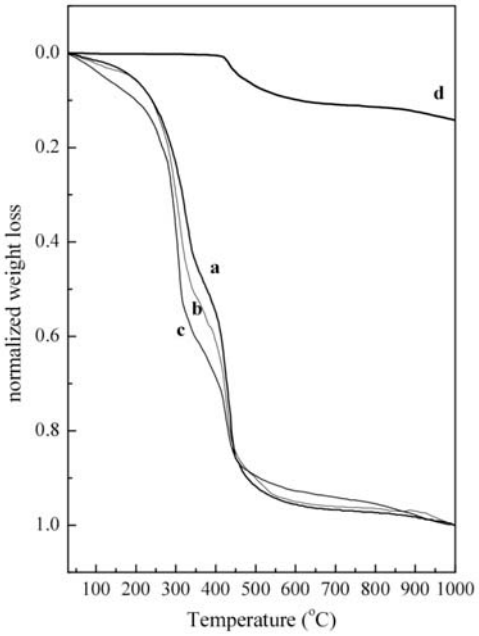

Fig. 4. Thermogravimetric curves of fluorapophyllite from Międzyrzecze. Heating rates as in Figure 3

All the analytical data for the Międzyrzecze apophyllite (Włodyka et al. 2004) confirm the suggestion that the amorphous layers coating apophyllite grains form a diffusion barrier restricting migration of H_2O molecules and, consequently, resulting in the second DTA endothermic peak. This is consistent with the model proposed by Ståhl (1993). The diffusion of H_2O through the apophyllite ring system from the outer parts of grains starts at about 160°C. The expulsion of a water molecule from the K-Ca sheets initiates the development of the amorphous phase. Subsequent water loss leads to permanent distortion of the puckered sillicate layers and the collapse of K-Ca coordination. The apophyllite grains become diphase with peripheral amorphous parts and crystalline interiors. The transition between them is controlled by outward diffusion of H_2O molecules.

The results of a series of DTA and TG runs using different heating rates are shown in Figures 3 and 4 (runs *a-c*). At lower heating rates, peaks I and II (Fig. 3) shift towards lower temperatures. The first peak is shifted more than the second one, extending the plateau between them; the amount of water expelled from the K-Ca sheets during the second stage decreases continuously with lower heating rates. Before run *d*, the sample was held at a temperature of 280°C over 27 hours; after recalculation this annealing corresponds to an averaged heating rate of 0.17°C/min. During this thermal experiment apophyllite showed a loss of 14.0 wt.% of water, whereas the remaining 2.31 wt.% during the run *d*. These results allow concluding that it is only at an infinitely slow heating rate that the diffusion barrier be overcome and the second endothermic peak disappears as all molecules of H_2O are removed in a one-step dehydration reaction. This was shown experimentally by Cavinato (1927). The DTA exothermic peak at about 800°C reflects the formation of wollastonite as a new crystal phase (Marriner et al. 1990).

As mentioned above, four Raman experiments were carried out in order to separate the excited modes/symmetry types for the polarization configurations presented in Table 3. It should be stressed here that compression of the spectra for $\bar{z}(y'y')z$ and $\bar{y}'(zz)y'$ geometry opened the possibility to separate the A_{1g} and B_{2g} modes.

Adams et al. (1981) discussed in detail the vibrational properties of apophyllite. The translatory motions of the K^+ and F^- ions are not visible in Raman spectra but can be observed in IR spectra (A_{2u} and E_u modes). For Ca, Si and O atoms, only four modes (A_{1g}, B_{1g}, B_{2g} and E_g) are active in Raman spectra and two modes (A_{2u} and E_u) in IR spectra. Water molecule vibrations contribute to all symmetry species and can be observed in both Raman and IR spectra.

TABLE 3

Raman scattering geometry used and excited modes

Geometry	Mode
$\bar{z}(y'y')z$	A_{1g}, B_{2g}
$\bar{z}(x'y')z$	B_{1g}
$\bar{y}'(zz)y'$	A_{1g}
$\bar{y}'(x'z)y'$	E_g

The measured polarized Raman spectra are shown in Figures 5 and 6. Spectral data for given experimental geometries, peak positions and related intensities are presented in Table 4. Compared to the findings of Adams et al. (1981), the data presented here

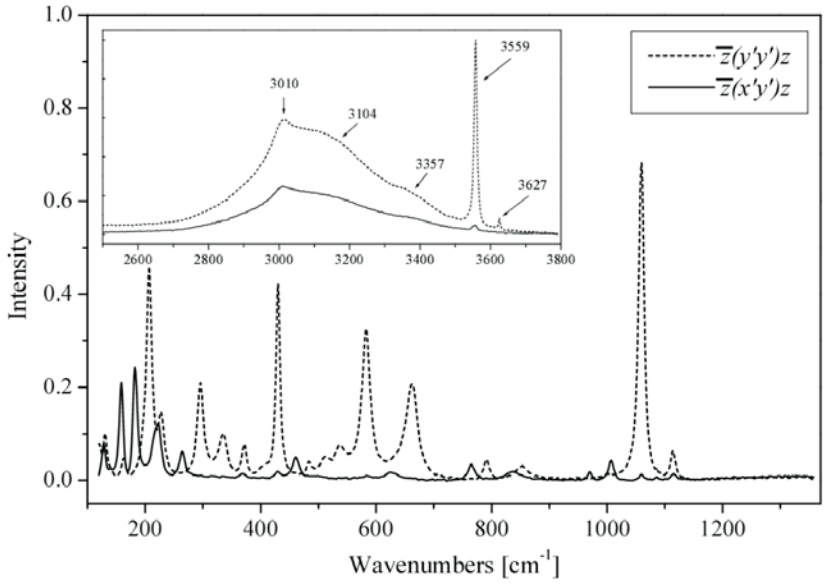

Fig. 5. Single-crystal Raman spectra of fluorapophyllite from Międzyrzecze at ambient temperature; $\overline{z}(y'y')z$ and $\overline{z}(x'y')z$ experiments

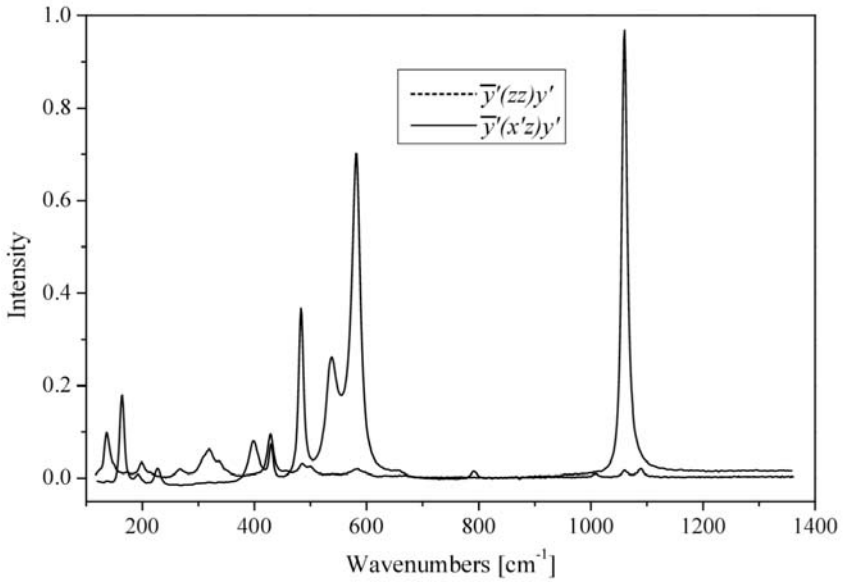

Fig. 6. Single-crystal Raman spectra of fluorapophyllite from Międzyrzecze at ambient temperature; $\overline{y}'(zz)y'$ and $\overline{y}'(x'z)y'$ experiments

TABLE 4

Raman wavenumbers and relative intensities of apophyllite from Międzyrzecze

Wavenumber ν [cm^{-1}]	Intensity [a)]			
	$\bar{z}(y'y')z$ A_{1g}, B_{2g}	$\bar{z}(x'y')z$ B_{1g}	$\bar{y}'(zz)y'$ A_{1g}	$\bar{y}'(x'z)y'$ E_g
1116.9	6.5	1.5		
1091.2				7.9
1062.3	77.6		100.0	
1010.8				7.3
1009.5		4.7		
972.5		2.0		
855.6	3.1			
840.2		2.1		
793.7	4.5		1.7	
767.5		3.7		
665.0	20.9			
629.6		1.7		
600.6				4.8
583.7	35.3		78.5	
541.5	6.5		27.5	
522.4	3.0			
502.9				3.6
487.3				3.5
485.5	3.1		41.0	
463.3		5.2		
459.6				3.3
432.5	47.6		8.4	
431.0				3.1
401.2	1.6		10.4	
374.0	7.0			
371.4		1.0		
341.8				2.5
336.8	9.9			
319.9				2.3
298.0	22.7			
269.8				1.9
266.7		5.8		
230.5	12.8		3.9	
225.8		9.6		
216.4				1.5
217.4		7.4		
209.2	51.1			
202.0				1.4
195.1			2.1	
184.7		24.2		
173.6				1.2
166.1	4.0		21.5	
160.9		22.5		
138.7				1.0
132.9	10.8			
130.7		6.8		
126.5				0.9
122.7	6.9			

[a)] Intensities are normalised to 100 for the strongest band.

show the intensive A_{1b} bands at 401.2 cm^{-1} and 195.1 cm^{-1}. Figures 5 and 7 show that the Raman and IR spectra in the ν(OH) region are very similar. In the apophyllite structure the water molecules are crystallographically equivalent (Colville et al. 1971). Neutron diffraction studies (Bartel et al. 1976; Princ 1971) reveal that there are two crystallographic positions H(1) and H(2) of hydrogen atoms. The first, broad complex band at about 3010 cm^{-1} (Raman spectra) and 3045 cm^{-1} (IR spectra) can be attributed to stretching vibrations of O(4)-H(1) hydrogen bond and the second, narrow band at 3559 cm (Raman and IR spectra) to O(4)-H(2) [O(4) — water oxygen] stretching. The complex shape of the first band probably reflects complex tones of ν(O4-H1) + ν_T, where T represents the translatory vibrations of water molecules (Ryskin et al. 1990). The present study has revealed a new, previously unrecorded, stretching vibration ν(OH) for apophyllite. The new band at 3627 cm^{-1} (Fig. 5) can be attributed to ν(OH) of the hydroxyl group which substitutes for F^- in the K-apophyllite structure. The H(1)O(4)H(2) bending modes are only active in the IR spectra and occur at about 1691 cm^{-1} (Fig. 7).

The mid- and far-IR spectra of apophyllite from Międzyrzecze are shown in Figure 7. The peak positions, related intensities and the band assignment according to Lazarev (1962) and Vierne et al. (1969) data are shown in Table 5. There are five bands

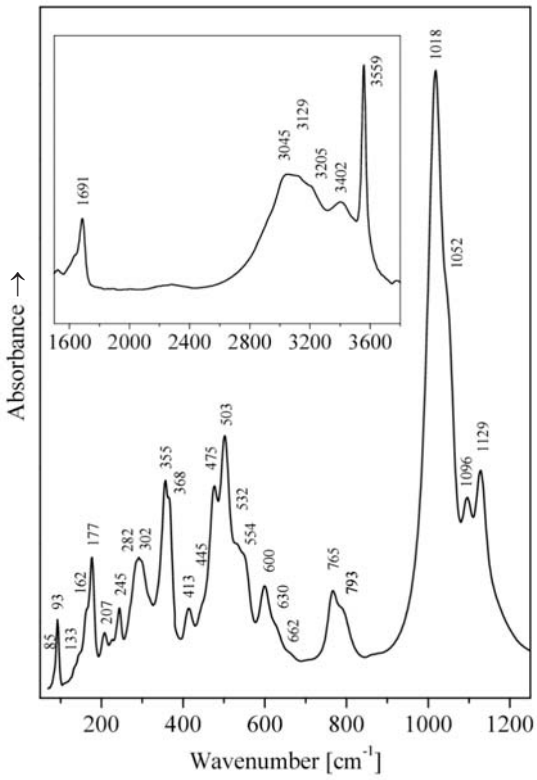

Fig. 7. Infrared absorption spectra of apophyllite from Międzyrzecze

TABLE 5

IR wavenumbers, relative absorbance and description of silicate vibrations of apophyllite from Międzyrzecze

Wavenumber ν [cm^{-1}]	Intensity[a)]	Silicate vibrations[b)]	Wavenumber ν [cm^{-1}]	Intensity[a)]
1128.8	w	A_{2u} ν_{as}(Si=O)	368.5	w
1095.7	w	E_u ν_s(Si=O)	354.8	w
1051.9	m	A_{2u} ν_{as}(Si-O)	346.0	vw
1017.9	vs	E_u ν_{as}(Si-O)	334.6	vvw
859.5	vvw		319.9	vvw
792.7	vw	E_u ν_s(Si-O-Si)	301.9	vw
764.4	vw		282.3	vw
661.8	vvw		268.3	vvw
629.8	vvw	E_u ν_s(Si-O-Si)	244.4	vvw
599.6	vw		225.2	vvw
554.3	w		207.3	vvw
532.3	vw	E_u δ_s(O=Si-O)	177.5	w
502.8	m	E_u δ_{as}(O=Si-O)	161.8	vw
474.5	w	E_u δ_s(O=Si=O)	145.6	vvw
444.7	vw		133.1	vvw
413.0	vvw		92.8	vw
390.6	vvw		84.7	vvw

[a)] Intensity in arbitrary units, normalised to the strongest band: vs — 100–80, s — 80–60, m — 60–40, w — 40–20, vw — 20–10, vvw — 10–0

[b)] ν — stretching, δ — bending vibrations

assigned to Si-O-Si bridged stretching modes between the SiO_4 tetrahedra. Thermal experiments on apophyllite (Włodyka et al. 2004) show that bands near 600 cm^{-1} (Fig. 7) completely vanish in the amorphous product of apophyllite dehydration, whereas bands between 700-800 cm^{-1} are observed in both forms. Thus, the bands near 600 cm^{-1} are due to Si-O-Si vibrations connected with the long-range order of the apophyllite structure and the remaining bands with the apophyllite ring system vibration. The bands in the region below 400 cm^{-1} can be associated with external motions of water and silicate sheets or with translatory motions of Ca^{2+}.

In an investigation of the sill intrusion mechanism, Einsele et al. (1980) showed that removal of seawater from the enclosing soft sediment creates space for the intruding magma. Later heat and mass transfer associated with the sill cooling creates chemically

distinct pore fluids infiltrating the host rocks and the intrusion and contributing to the development of the contact aureole. The type of the permeability field in the host rocks mainly controls the scale and extent of contact aureole. As the sill cools and solidifies, fracturing occurs, effective permeability increases and fluid flow into the sill interior is promoted. Precipitation or metasomatic reactions driven by the advection of thermal energy and fluids out of equilibrium with the local environment, occur mainly in highly permeable zones. At Międzyrzecze, they were mainly confined to the upper, marginal part of the sill. The contact aureole contains such metamorphic minerals as pectolite, datolite, diopside, Ti-garnets, strontianite, barite, fluor-apophyllite and fluor-apatite. Fluorite and witherite have been identified as fissure filling in the contact aureoles of the picrite-teschenite sills from northern Moravia (Kudělásek et al. 1987, 1990). An identical set of minerals occurs in the contact aureole of an 11-meter monchiquite sill in Louisiana (Dutrow et al. 2001). For this sill, a series of coupled heat and mass transport calculations for different type of host-rock permeability field (homogeneous, anisotropic and layered) were presented. They show that the thermal (metamorphic) pulse was very short-lived; it waned in ~ 3 years with a return to background temperatures completed in about 10 years. The maximum temperatures (250–350°) estimated by Dutrow et al. (2001) for the pectolite zone are similar to those reached at Międzyrzecze (Wieser 1971; Włodyka 1998).

The mode of apophyllite and fluorite occurrence in fissures suggests the following reactions:

(a) $4\ CaCO_3 + 8\ SiO_2 + 8H_2O + K^+ + HF = KCa_4Si_8O_{20}(F,OH) \cdot 8H_2O + 4CO_2 + H^+$

(b) $CaCO_3 + 2HF = CaF_2 + CO_2 + H_2O$

These reactions imply a late, low-temperature influx of F-enriched fluids with increasing activity of potassium cations. Because apophyllite and fluorite occur only in the contact aureole of the picrite sills rich in phlogopite, selective leaching of these aureoles released necessary elements for the precipitation of apophyllite (open-spaces filling type) and fluorite.

Acknowledgements. The authors are grateful for carrying out instrumental analyses to Dr G. Bzowska (XRD), Dr M. Sitarz (IR), and to Mr. B. Ptak (TG, DTA). We are especially grateful to Dr Padhraig Kennan for critical reading and help in preparation of the English text.

REFERENCES

ADAMS D.M., ARMSTRONG R.S., BEST S.P., 1981: Single-crystal Raman spectroscopic study of apophyllite, a layer silicate. *Inorg. Chem*. 20, 1771–1776.

AKIZUKI M., KONNO H., 1985: Internal texture and abnormal optical property of apophyllite. *N Jb. Miner. Abh.* 151, 99–115.

BARTEL H., PFEIFER G., 1976: Neutronenbeigungsanalyse des Apophyllite $KCa_4(Si_4O_{10})_2(F/OH) \cdot 8H_2O$. *N Jb. Miner. Mh.* H. 2, 58–65.

BELSARE M.R., 1969: A chemical study of apophyllite from Poona. *Mineral. Mag*. 37, 288–289.

BORISENKO Y.A., 1982 : Propagation and property of apophyllite. *Miner. Zhurn*. 4, 53–60 (in Russian).

CAVINATO A., 1927: Sulla disidratazione dell apofillite. *Atti Lincei* 5, 907–910.

CHAO G. Y., 1971: The refinement of the crystal structure of apophyllite. II. Determination of the hydrogen positions by X-ray diffraction. *Am. Miner*. 56, 1234–1242.

COLVILLE A.A., ANDERSON C.P., 1971: Refinement of the crystal structure of apophyllite. I. X-ray diffraction and physical properties. *Am. Miner*. 56, 1222–1233.

DUNN P.J., ROUSE R., NORBERG J.A., 1978: Hydroxyapophyllite, a new mineral, and a redefinition of the apophyllite group. I. Description, occurrences, and nomenclature. *Am. Miner*. 63, 196–199.

DUTROW B.L., TRAVIS B.J., GABLE C.W., HENRY D.J., 2001: Coupled heat and silica transport associated with dike intrusion into sedimentary rock: Effects on isotherm location and permeability evolution. *Geochim. Cosmochim. Acta* 65(21), 3749–3767.

EINSELE G., GIESKES J.M., CURRAY J., 1980: Intrusion of basaltic sills into highly porous sediments, and resulting hydrothermal activity. *Nature* 283, 441–445.

FLEMING T.H., FOLAND K.A., ELLIOT D.H., 1999: Apophyllite $^{40}Ar/^{39}Ar$ and Rb-Sr geochronology: Potential utility and application to the timing of secondary mineralisation of the Kirkpatrick Basalt, Antarctica. *J. Geophys. Res.* 104, 20081–20095.

KOSTOV I., 1975: Apophyllite morphology as an example of habit modification of planar crystals. *N. Jb. Miner. Mh.* 123(2), 128–137.

KUDĚLÁSEK V., MATÝSEK D., KLIKA Z., 1987: Datolite occurrences in the area of rocks of the teschenite association (northern Moravia). *Čas. Mineral. Geolog.* 32(2), 169–174 (in Czech).

KUDĚLÁSEK V., MANDUR M.A., MATÝSEK D., 1989: Occurrence of witherite and barite in teschenitic rocks. *Čas. Mineral. Geolog.* 34(2), 205–207 (in Czech).

KUDĚLÁSEK M., KUDĚLÁSEK V., MATÝSEK D., 1990: Zeolites in picrite of the teschenite association at the locality Hončova hůrka near Příbor (northern Moravia). *Čas. Mineral. Geolog.* 35(3), 317–321 (in Czech).

LAZAREV A.N., 1962: Vibrational spectra and structure of silicates. AN SSSR, Leningrad.

MARRINER G.F., TARNEY J., LANGFORD J.I., 1990: Apophyllite group: effect of chemical substitutions on dehydration behaviour, recrystallization products and cell parameters. *Mineral. Mag*. 54, 567–577.

MATSUEDA H., MIURA Y., RUCKLIDGE J., 1981: Natroapophyllite, a new orthorhombic sodium analog of apophyllite. I. Description, occurrence, and nomenclature. *Am. Miner*. 66, 410–415.

MIURA Y., KATO T., RUCKLIDGE J., MATSUEDA H., 1981: Natroapophyllite, a new orthorombic sodium analogue of apophyllite. II. Crystal structure. *Am. Miner*. 66, 416–423.

PECHAR F., 1987: An X-ray diffraction refinement of the crystal structure of natural apophyllite. *Cryst. Res. Technol*. 22, 1041–1046.

PRINCE E., 1971: Refinement of the crystal structure of apophyllite. III. Determination of the hydrogen positions by neutron diffraction. *Am. Miner*. 56, 1243–1251.

RYSKIN Ya.I., STAVITSKAYA G.P., 1990: Asymmetry of the water molecule in crystal hydrates: IR spectra of dioptase and apophyllite. *Izv. AN SSSR Ser. Khim*. 8, 1778–1782 (in Russian).

SAHAMA Th.G., 1965: Yellow apophyllite from Korsnäs, Finland. *Mineral. Mag*. 34, 406–415.

STÅHL K., KVICK Å., GHOSE S., 1987: A neutron diffraction and thermogravimetric study of the hydrogen bonding and dehydration behavior in fluorapophyllite, $KCa_4Si_8O_{20}F \cdot 8H_2O$, and its partialy dehydrated form. *Acta Cryst*. B43, 517–523.

STÅHL K., 1993: A neutron powder diffraction study of partially dehydrated fluorapophyllite, $KCa_4Si_8O_{20}F \cdot 6.9H_2O$. *Eur. J. Mineral*. 5, 845–849.

TAYLOR H.F.W., NÁRAY-SZABÒ ST., 1931: The structure of apophyllite. *Zeits. Kristallogr*. 77, 148–56.

VIERNE R., BRUNEL R., 1969: Spectres de réflexion infrarouge de minéraux monocristallins ou en poudre. I. *Bull. Soc. Fr. Minéral. Cristallogr*. 92, 409–419.

WIESER T., 1971: Przeobrażenia egzo- i endokontaktowe związane z cieszynitami Karpat fliszowych Polski. *Kwart. Geol.* 15, 901–920.

WŁODYKA R., KAPUSTA J., GALUSKIN E., 1998: Datolite from the environs of Cieszyn and Bielsko-Biała in the Polish Carpathians (the type area of the teschenite association). *Arch. Miner*. 51, 1–2, 273–287.

WŁODYKA R., BZOWSKA G., WRZALIK R., 2004: The thermal behaviour of fluorapophyllite from the Międzyrzecze sill near Bielsko-Biała in the Polish Carpathians. *N. Jb. Miner. Mh.* (in press).

Roman WŁODYKA, Roman WRZALIK

APOFYLLIT Z SILLU W MIĘDZYRZECZU KOŁO BIELSKA-BIAŁEJ, OBSZAR TYPOWY ASOCJACJI CIESZYNITOWO-PIKRYTOWEJ

Streszczenie

W stropowej partii sillu pikrytowego w Międzyrzeczu Górnym koło Bielska-Białej stwierdzono występowanie apofyllitu (Fot. 2 i 3). Minerał ten stanowi składnik wypełnienia złożonych żył tnących ciało endoskarnu pektolitowego (Fot. 1).

Apofyllit poddano analizie chemicznej (Tab. 1), badaniom rentgenowskim (Fig. 1, Tab. 2), termicznym (Fig. 3 i 4), spektroskopii absorpcyjnej w podczerwieni (Fig. 7, Tab. 5) oraz badaniom ramanowskim (Fig. 2, 5 i 6, Tab. 3 i 4).

Wyniki analizy chemicznej pozwoliły zaliczyć badany minerał do fluorapofyllitów zawierających niewielkie domieszki Na oraz Al. Wykazuje on symetrię tetragonalną; oznaczone parametry komórki elementarnej mają następujące wartości: a = 8,974(2) Å, c = 15,798(6) Å. Badany minerał nie wykazuje obecności anomalii optycznych typowych dla apofyllitów z podwyższonym udziałem Al_2O_3 oraz Na_2O. Własności termiczne apofyllitu (obecność dwóch pików endotermicznych na krzywych DTA) można wyjaśnić obecnością bariery dyfuzyjnej (amorficznego produktu dehydratacji apofyllitu) w zewnętrznych partiach jego ziaren, która zaczyna się tworzyć w temperaturach powyżej 160°C.

Występowanie apofyllitu w Międzyrzeczu oraz w północnych Morawach jest związane z sillami pikrytu bogatymi we flogopit. Roztwory hydrotermalne oddziałujące z tymi skałami wzbogaciły się w składniki niezbędne do krystalizacji apofyllitu na powierzchniach szczelin tnących endoskarn pektolitowy.

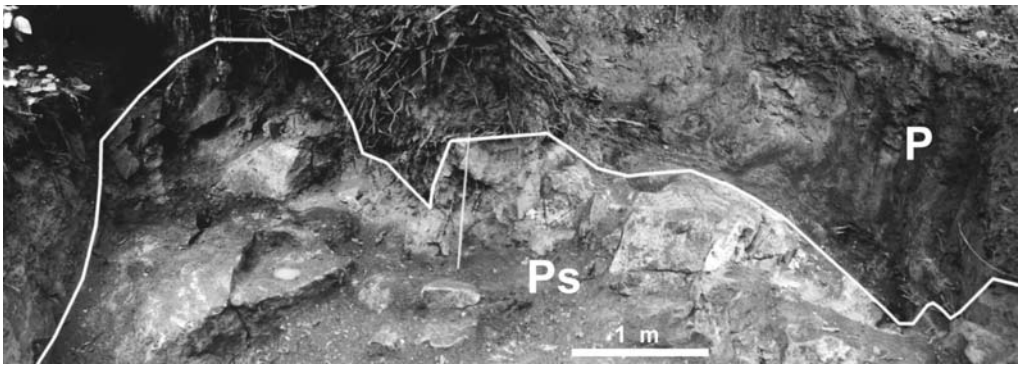

Phot. 1. Lenticular body of pectolite endoskarn overlain by strongly altered picrite in the upper part of the Międzyrzecze sill.
P — picrite, Ps — pectolite skarn

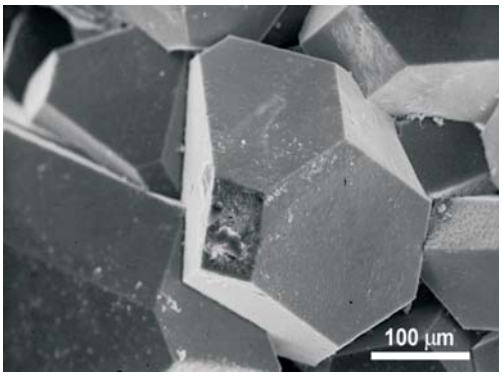

Phot. 2. Typical bipyramidal apophyllite from Międzyrzecze with (001) faces exhibiting very rough and dull surfaces

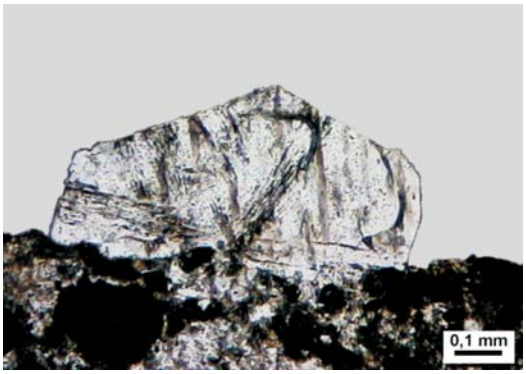

Phot. 3. Vertical section (in transmitting light) through a bipyramidal crystal of apophyllite showing bunches of dislocations oriented perpendicular to growth layers. A perfect (001) cleavage is also visible